*Acta Cryst.* (1972). A**28**, 1

# Si (111) Surface Structures by Glancing Incidence High-Energy Electron Diffraction

BY J. F. MENADUE*

*Department of Materials Science and Engineering, Cornell University, Ithaca, New York* 14850, *U.S.A.*

(*Received* 9 *October* 1970)

The structures which form on the (111) surface of a silicon single crystal have been examined by glancing incidence high-energy electron diffraction under ultra-high vacuum conditions. A quantitative measurement of the intensities of the *hhh* systematic set of Bragg reflections from the 2nd to the 7th order was observed as a function of azimuthal angle, rocking angle and temperature. In particular, the intensity of the *hhh* reflections was measured at crystal azimuths which minimize the non-systematic *n*-beam interference. These 'azimuth-independent' rocking curves for the $1 \times 1$, 7 and $\sqrt{19}$ structures are compared and discussed, to explore the possibilities of obtaining structural information for both the surface and the bulk by the glancing incidence high energy technique. The data are suitable for comparison with the calculations of an *n*-beam dynamical theory as it is developed and adapted to the Bragg case.

The refractive shift of the Bragg peaks yielded a value of $12{\cdot}0 \pm 0{\cdot}4$ volts for the mean inner potential of silicon.

## Introduction

The suitability of high-energy electron diffraction as a tool to study surface structure was recognized many years ago by Finch & Wilman (1937). More recently the dynamical diffraction theory has been developed to the point where accurate structure analysis of samples thin enough for the electron beam to penetrate has become possible (Cowley, 1967, 1969). It is not unreasonable to expect that some of the procedures developed for the transmission case can be extended to study the structures which form on low-index single-crystal surfaces.

As Miyake & Hayakawa (1970) have recently pointed out, there are many similarities in the multiple beam interference effects observed by glancing incidence high energy (HEED) and low energy (LEED) electron diffraction from single crystals. There is however a considerable difference in the approach to the dynamical theory, arising mainly from the very strong elastic and inelastic interactions of the low-energy electrons (Jones & Strozier, 1969; Strozier & Jones, 1970) which penetrate only a few atom layers, even at near normal incidence. High-energy electrons in the range of 10 to 100 keV penetrate considerably further, and scatter through low angles. Nevertheless for the lowest order diffracted beams, which occur at a glancing angle of incidence of about 1°, the interaction is concentrated in a surface region not much deeper than for LEED.

### (*a*) *Structure normal to the surface*

The limited beam penetration of both techniques results in the usual triperiodic reciprocal-lattice points being drawn out to form almost continuous rods normal to the real crystal surface. The intensity distribution along the rods is not the same, however, but depends on the energy, which affects the scattering mechanism and the depth of crystal contributing. It is not at all usual to find that there is only one reciprocal-lattice point apart from the origin which is close to the Ewald sphere, and thus only one diffracted beam (Siegel & Menadue, 1967). There will be strong dynamical interactions between several simultaneously excited diffracted beams.

The possibility of interpretation at higher energies in terms of already well developed *n*-beam theory, together with greater penetration and higher resolution makes glancing incidence HEED a practical tool to examine the structure in a direction normal to the crystal surface. If there is an overlayer with a different periodicity which is thin enough to be penetrated, both sets of Bragg peaks will be present simultaneously in the diffraction pattern (Newman & Pashley, 1955). Amorphous layers up to tens of Å thick can be penetrated, and the interface with the periodic substrate examined. Thus the different structures which form on a crystal surface can be compared to investigate the changes in periodic and atomic structure normal to the surface, and the differences between these surface structures and that of the bulk crystal.

### (*b*) *General structure analysis*

For both the low- and the high-energy techniques, the coherence width in the plane of the surface is large enough that a cross section through the reciprocal lattice in a plane parallel to the surface (*i.e.* normal to the reciprocal-lattice rods) reveals patterns with a similar geometry. The diffraction pattern displayed in and between the zero and first Laue zones by the high-energy technique may be readily converted to that displayed by the low-energy technique at near normal incidence.

The geometry of diffraction reveals the periodicity of the crystal, from which the size and orientation of the unit surface mesh or unit cell can be determined. Pos-

* Present address: Institut für Elektronenmikroskopie am Fritz-Haber-Institut der Max-Planck-Gesellschaft, 1 Berlin 33, Faraday Weg 4–6, Germany.

sible models of the position and nature of each atom in the unit cell may be inferred, but they are generally not unique. It is the purpose of this and a following paper in part to explore the experimental possibilities of obtaining structural information from quantitative intensity measurements made on glancing incidence high-energy electron diffraction patterns, obtained under ultra-high vacuum conditions. An *n*-beam dynamical theory was developed simultaneously for the Bragg case of diffraction by Colella (1972), and the calculated intensities will be compared with those observed in a following paper, Colella & Menadue (1972).

In addition, the structures and morphological changes occurring on the Si(111) surface as it is cleaned serve to demonstrate that the glancing incidence method is particularly appropriate for this kind of observation.

### The diffraction camera

The diffraction camera is of the now usual stainless steel, bakeable ultra-high vacuum construction and has been described in Siegel & Menadue (1967). As in Fig. 1, a 40 keV electron beam was incident on the specimen at an angle variable from 0 to 4° by tilting the specimen, which could be independently rotated without changing the tilt angle. The beam shape was optimized to a flat ribbon 300$\mu$ wide by 45$\mu$ high by an aperture before the specimen, and focused onto a fluorescent screen by a single magnetic lens. The vertical beam divergence, *i.e.* normal to the specimen surface, was $1{\cdot}4 \times 10^{-4}$ rad, and the full beam current of $7 \times 10^{-8}$ amp fell onto an 8 mm diameter surface for incidence angles down to 0·3°, as required for quantitative intensity measurements. Diffracted intensities were measured by a Faraday cup, with an entrance aperture shaped according to the needs of the experiment. Current sensitivity was routinely less than $10^{-13}$ amp, allowing reflected intensities as low as $10^{-6}$ of the incident intensity to be recorded.

The specimen was heated by electron bombardment from beneath with a beam energy of up to 2 kV and 100 mA available. The temperature was stabilized by feedback from a W–W 26% Re thermocouple inserted in a $\frac{1}{2}$ mm diameter hole 2 mm deep in the side of the specimen. The temperature of the diffracting surface as measured with an infrared radiation thermometer was found to be in good agreement with the thermocouple reading.

The data were taken without an energy filter, so that the peak intensities as recorded are about 50% elastic (Colella & Menadue, 1971). The inelastically scattered components will need to be filtered out when comparisons with theory are attempted to an accuracy better than a factor of two.

### The specimen

It was desirable that the specimen come as close as possible to the simplest model, that of a perfect semi-infinite crystal, to minimize the complexity of this initial investigation. Silicon was chosen, its crystalline perfection having been well established by X-ray methods. Polishing and cleaning techniques were well known, in particular that of cleaning by heating in high vacuum (Allen, Eisinger, Hagstrom & Laur, 1959). It seemed likely that this method would result in surfaces which were suitably flat and clean, the high atomic density (111) surface being least likely to facet to any other during the cleaning procedure. The surface structures have been extensively studied by other means, chiefly LEED. References are well listed in Russell (1970).

The original silicon stock was *n*-type with a resistivity of 200$\Omega$.cm, and a dislocation density of $< 100/\text{cm}^2$. Slabs 26 mm in diameter were cut and polished to within 0·1° of the (111) surface, and smaller discs 8 mm in diameter were cut from the center of the slabs to obtain suitably flat specimens. The polished surfaces were examined under an optical interferometer. Acceptable surfaces were slightly dome shaped, the angular devia-

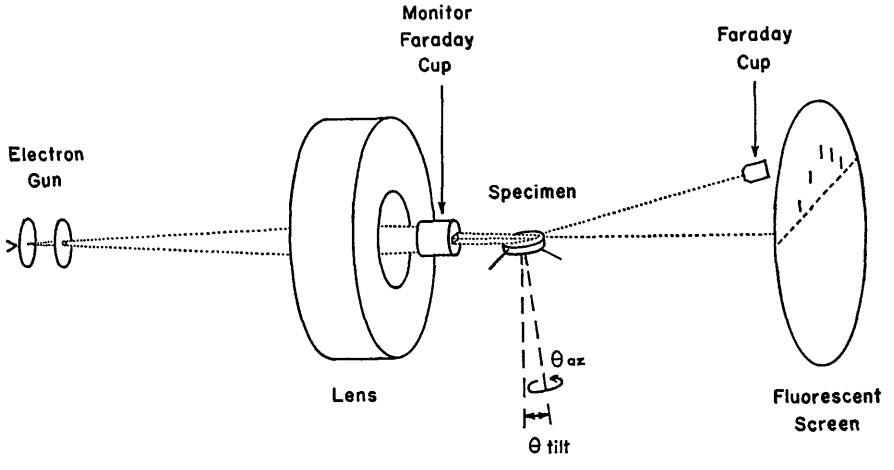


Fig. 1. Glancing-incidence high-energy electron diffraction camera.

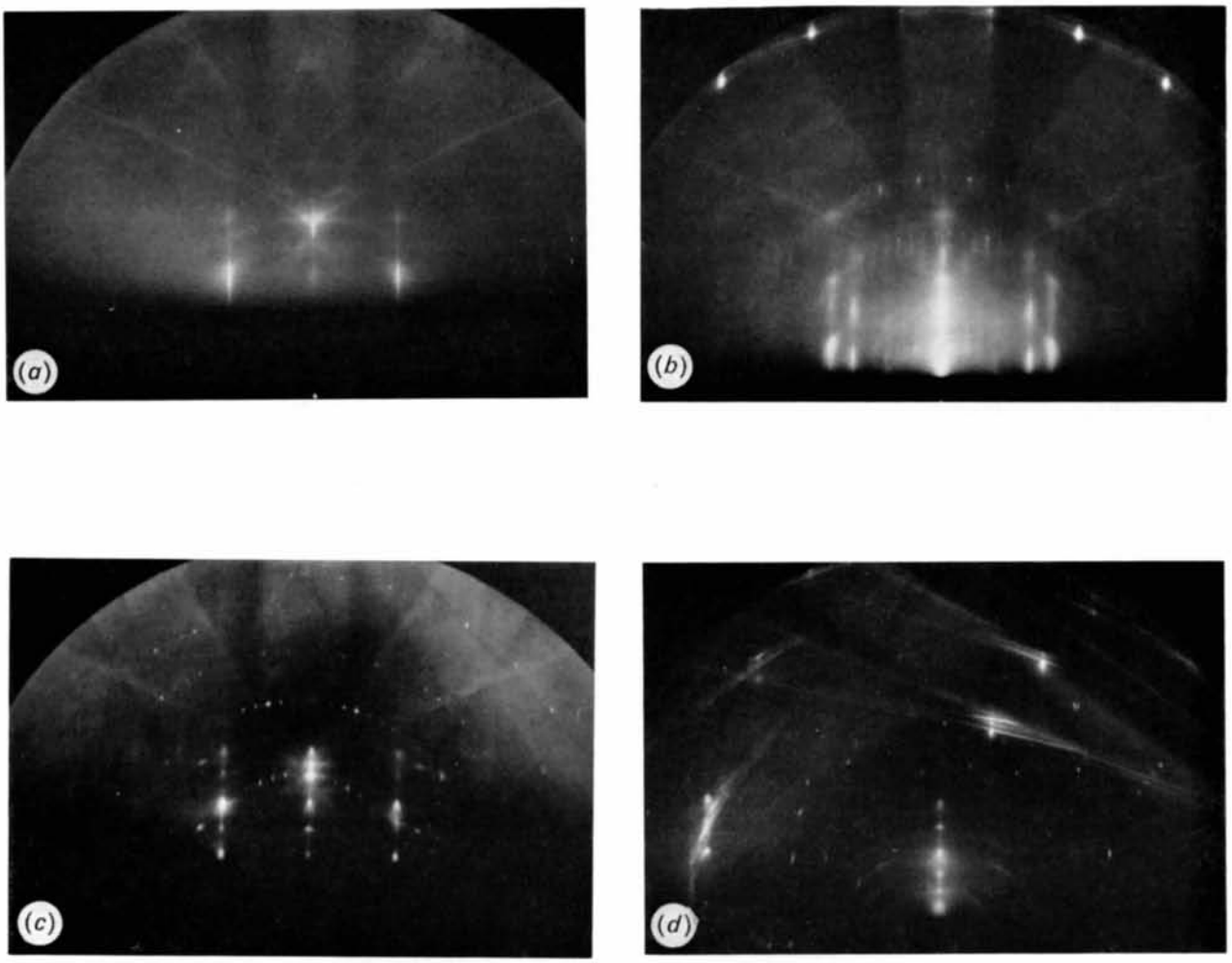


Fig. 2. (*a*) Original Si(111) surface, before cleaning. Az⟨$\bar{2}$11⟩. Tilt 444. (*b*) After heating to 785 °C. At room temperature. Az⟨$\bar{2}$11⟩. Tilt 222. (*c*) After heating to 1100 °C. At room temperature. Az⟨$\bar{2}$11⟩. Tilt 444. (*d*) After heating to 1100 °C. At room temperature. Note 'arrowheads' and Sherrer rings. Az 12° off ⟨$\bar{1}$10⟩. Tilt 222.

[*To face p.* 2

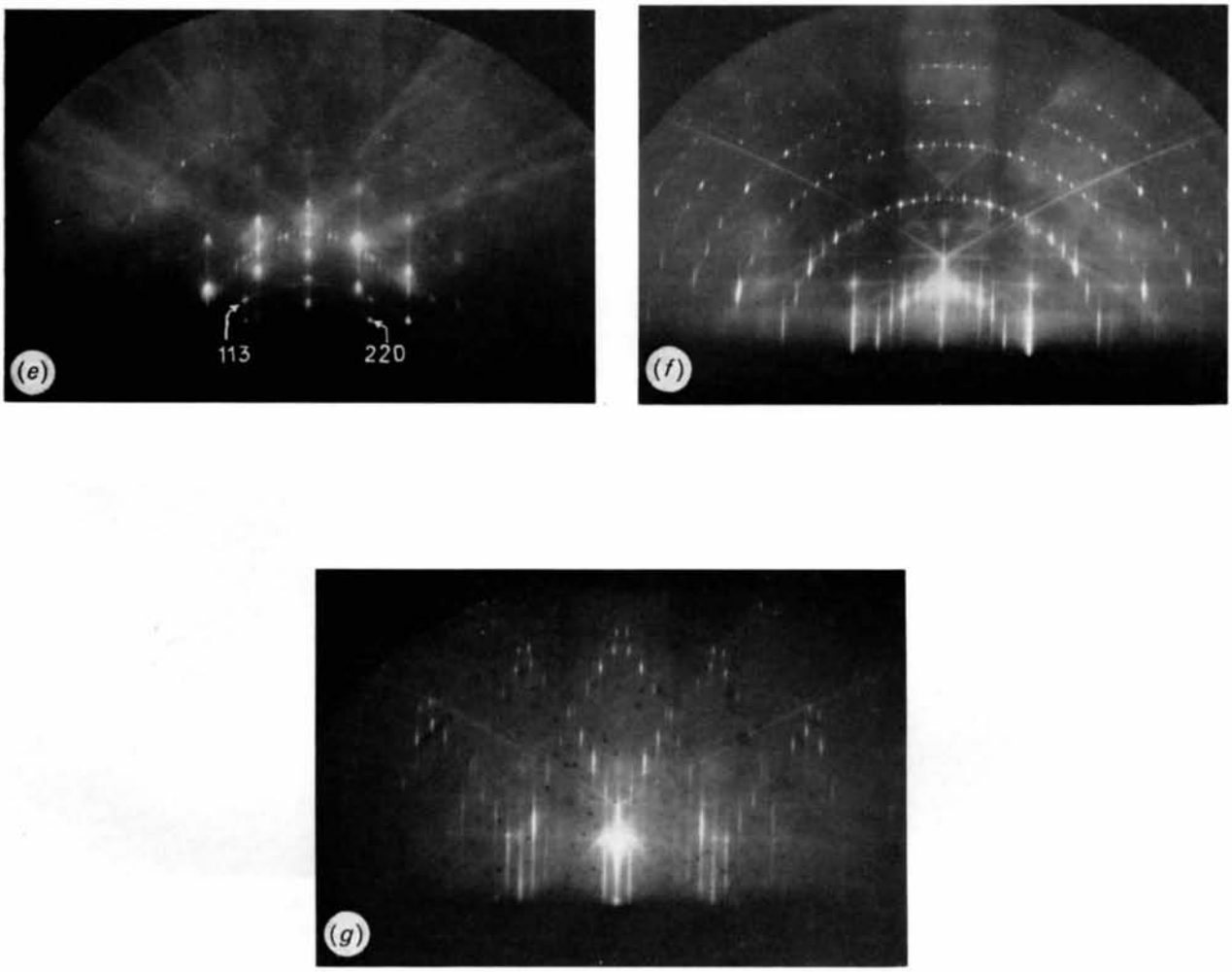


Fig. 2. (*cont.*) (*e*) After heating to 1100°C. At room temperature. Note cross-grating pattern of 'arrowheads'. Az $\langle\bar{1}10\rangle$. Tilt near 444. (*f*) After heating to 1150°C. At room temperature. 7th-order pattern. Az $\langle\bar{2}11\rangle$. Tilt 333. (*g*) Si(111) 19th-order pattern. Az $\langle\bar{2}11\rangle$. Tilt 333.

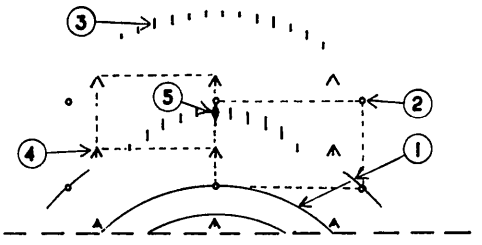


•ooo

Fig. 3. Schematic diagram of Fig. 2(*c*) to show (1) Scherrer ring pattern, from disoriented $\beta$-SiC; (2) extra side streaks from oriented $\beta$-SiC; (3) weak 7th order pattern, from a flat surface; (4) cross grating set of 'arrowheads', from Si lattice; (5) 444 Bragg reflection, from a flat surface.

tion over a 2 mm diameter being less than $10^{-4}$ radian. This was satisfactory since when the rocking curve widths were of this order at high angles of incidence, the incident electron beam illuminated an area considerably less than 2 mm in length. Some specimens were polished by a chemical-mechanical method, using 'Syton' from Monsanto Chemical Co., and others with $0{\cdot}05\mu$ alumina and water. The specimens were not further chemically etched before mounting in the diffraction camera, as this unnecessarily roughens the surface. Instead, the layer damaged by polishing was thermally etched away in the ultra-high vacuum environment. In this way the process could be followed by electron diffraction and terminated as soon as the specimen was effectively clean, to ensure that the final surface would be as flat as possible as required for quantitative intensity measurements to be significant.

Although specimens are polished to seem perfectly flat by optical standards, it is quite possible that the subsequent cleaning procedures may result in the formation of pits, facets or undulations on the surface which will modify the intensities of the beams diffracted from an otherwise still optically flat surface. There will be interference effects between those parts of the electron beam which enter or leave the surface through adjacent areas at different levels (or at slightly different angles) within the coherence width, when the step dimensions are only a few atom plane spacings high (Lander, Gobeli & Morrison, 1963). It is not practicable to allow for such interference in calculating the intensities at this initial stage. Fortunately departures from flatness with facet size approaching the extinction distance, or larger are readily observable (Kato, 1952; Menadue & Siegel, 1969). At 40 keV, with glancing incidence, facets of the order of 100 Å or larger are detected by the appearance of new streaks in the diffraction pattern which are not normal to the nominal polished surface. These are seen when the resulting 'Stacheln' in the reciprocal lattice lie parallel to the surface of the Ewald sphere.

Undulations in the surface, a common cause of long streaks, were readily detected. The instrumental contribution to the length of the observed streaks can be conveniently measured in terms of the angle subtended at the specimen. In the present case it arises from the sum of the divergence of the incident beam, $1{\cdot}4\times10^{-4}$ rad and the focused spot size, equivalent to $1{\cdot}6\times10^{-4}$ rad. The contribution from beam voltage variations was negligible. Thus structures which were formed on flat surfaces of undistorted crystals were characterized by the shortness of the streaks, approaching the above total of $3\times10^{-4}$ rad.

### Initial cleaning

The geometrical changes observed during the initial heating of all new specimens polished by either of the previously mentioned methods are shown in Fig. 2. Fig. 2(*a*) is from an original specimen, unheated except for a 12 hour 300°C bakeout. It looks remarkably clean, in that the features present are only those that would be expected from a perfectly flat Si(111) specimen, and the refractive shifts are exactly equal to those measured later on a clean, flat surface. The Bragg intensities are low, however, and the background intensity is high, the first indication of the presence of a thin, amorphous overlayer, through which the beam can penetrate to be diffracted in the underlying silicon. Under somewhat similar conditions Sewell (1970), with characteristic X-ray spectrometry has shown the presence of carbon and oxygen on the Si(111) surface. Thin amorphous overlayers are difficult to detect visually by HEED, since even the refractive shift of the Bragg reflections toward the shadow edge remains unaltered by the overlayer (Tull, 1951) regardless of a mean inner potential which is most probably different to that of silicon. The point to emerge here is that the underlying silicon seems to be well ordered right up to the interface with the amorphous overlayer.

In Fig. 2(*b*), the specimen had been heated to 785°C, when extra side streaks appeared in all low-index zones. These belong to crystallites of a similar crystallographic type, but with a smaller lattice constant, oriented parallel to the silicon substrate. The streak spacing corresponds to a unit cell side of 4·35 Å which is that of $\beta$-SiC, the cubic form. The breadth of the streaks indicates that the crystallites have lateral dimensions of the order of 20 Å at this stage.

The temperature was increased in increments of about 50°C, cooling between each step. In Fig. 2(*c*), the specimen has been heated to 1100°C for 30 seconds. There are four distinct patterns superimposed here, more readily separated in the schematic of Fig. 3.

First, there is a Scherrer ring pattern seen best in Fig. 2(*d*). There were 8 rings visible in this pattern, which belongs to a face-centered cubic lattice with the unit cell size of $\beta$-SiC again. The randomly oriented crystallites responsible for these rings have an average dimension of about 70 Å, as determined from the width of the rings.

Second, the extra side streaks have decreased in size to a set of spots, which have not been displaced by refraction, and fall on the appropriate rings. Thus, the electron beam is passing through asperities formed by $\beta$-SiC crystallites protruding above the nominal surface plane. All of these spots are drawn into short arcs, owing to a slight misorientation by $\pm 10^{-3}$ rad of these crystallites, which otherwise remain oriented on the bulk structure. In the $\langle 110 \rangle$ zone [Fig. 2(*e*)] the 113 and 220 spots appear mirrored across the 111 axis due to twinning. The appearance of the spot pattern is not unlike that from a needle texture of the first kind (plate XIX, Vainshtein, 1964). Needles of $\beta$-SiC have been found previously by Abbink, Broudy & McCarthy (1968) in replicas stripped from Si(111) after annealing at 900 °C for 1 hour, on (111) substrates after etching in hydrogen by Miller, Watelski & Moore (1964) and have been observed with HEED by Henderson, Polito & Simpson (1970).

Third, a weak 7th-order pattern appeared when the specimen was cooled suggesting that part of the surface now has the structure sometimes associated with a clean (111) surface in LEED investigations. The inner (zero Laue) zone of this pattern consists of short streaks lying on a circle. The shortness of the streaks shows that the pattern has come from a very flat surface, or more probably from many facets, all strictly parallel to each other. The specularly reflected Bragg spot (in this case the 444) also falls exactly on this circle, showing that the facets are indeed parallel to the (111) crystal planes.

There is a fourth set of spots shaped like arrowheads, falling on an extensive cross-grating pattern similar to those observed in transmission diffraction. There is no discernible refractive shift for this pattern, which yields the unit-cell dimensions of Si both horizontally and vertically, when measured from the tip of the arrow. The length of the barbs on the arrowheads varies as the specimen is rotated. This, together with the angle of about 40° in the arrowheads, is consistent with a surface morphology containing features which in essence resemble truncated cones with predominant (211) and perhaps (331) facets, as shown in Fig. 4. This morphology is strikingly similar to that observed during the epitaxic growth of silicon on (111) silicon by vapour deposition, as in Fig. 4 of Abbink, Broudy & McCarthy (1968). A similar transport phenomenon may be occurring here as the SiC sublimes away. It could also be related to the wavy stepped surface seen after heating for a considerable time at a slightly higher temperature, by Russell & Haneman (1967). The barbs can be ascribed to the effects of refraction, as follows. The beam traverses the crystal through the cross hatched areas along the outer edges of the cone, which are sufficiently rounded so that the beam suffers varying amounts of refractive deviation. The deviation of the diffraction spot is in the plane containing the normals to this curved surface. The beam which has penetrated deeply and has passed through well inclined surfaces will suffer negligible deviation, and will form the tip of the arrowhead. The beam which has penetrated very little crystal will enter and leave at more glancing angles, and will suffer a considerable deviation to form the barbs of the arrowhead. Thus, as observed, the barbs are longer for low order reflections, for which the range of refractive deviation is greater.

Finally, heating to 1150 °C results in the vanishing in about 1 minute of all signs of SiC and of the cross grating arrowhead pattern too, leaving an apparently clean and flat surfaced Si pattern while hot. Strong 7th- or 19th-order patterns appear on cooling as in Fig. 2(*f*) and (*g*). The SiC has sublimed away, and some carbon may have diffused back into the bulk. The silicon surface has remained essentially flat. The SiC cycle can be repeated if the specimen is re-exposed to the atmosphere. Once removed at 1150 °C however it does not return with any further heat treatment. It has been shown by Henderson & Polito (1969) that although there is carbon impurity in the silicon, it could not diffuse out quickly enough to form the SiC observed. Also that the carbon could not come from traces of hydrocarbons in the vacuum. Using characteristic X-ray spectrometry Sewell (1970) has found carbon and oxygen on Si surfaces, even after careful cleaning procedures. It appears that a surface layer is absorbed from the atmosphere after polishing, in an amorphous form so that it is not visible in the diffraction pattern until heating causes the SiC crystallites to grow.

### Geometry of flat surface diffraction patterns

On the two specimens polished in Syton it was possible to form three surface structures by heat treatment alone, with no exposure to gases or ions other than the usual residuals in the ultra-high vacuum environment. The gases are CO, $CO_2$, $H_2$ and Ar to a total pressure of $10^{-9}$ torr. Strong 7th- and 19th-order periodicities could be obtained easily and interchangeably, as well as a $1 \times 1$ pattern. The 19th-order pattern was most easily obtained by cooling rapidly from any temperature above 700 °C. Temperatures near 700 °C had to be maintained for several minutes before cooling in order to get strong patterns. Above 570 °C the 19th-order pattern faded in a few minutes leaving a bright, sharp $1 \times 1$ pattern similar to Fig. 2(*a*), but with a lower

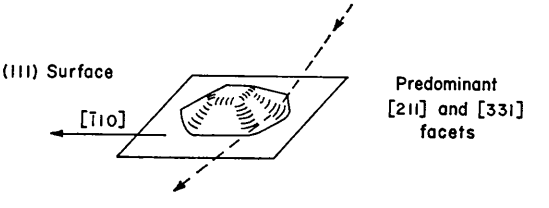


Fig. 4. Truncated cones of silicon which could produce the observed arrowhead shapes in the diffraction pattern, by refraction through the curved sides.

background, which remained at room temperature. It resembled what one would expect from a perfect Si(111) surface. Heating between 600 °C and 670 °C resulted in a 7th-order pattern which increased in strength for about 15 minutes, and became stronger still on cooling to room temperature. The 7th-order faded in a few seconds at 700 °C, leaving a clean looking pattern at room temperature. The above temperature cycling agrees well with that of Schlier & Farnsworth (1959) and van Bommel & Meyer (1967). One would not expect that all three structures observed were of 'clean' surfaces; yet it is not possible to tell from observation which one, if any, is clean. The $1 \times 1$ case may have a superstructure of impurity atoms on it, or a thin amorphous layer as must exist for Fig. 2(*a*).

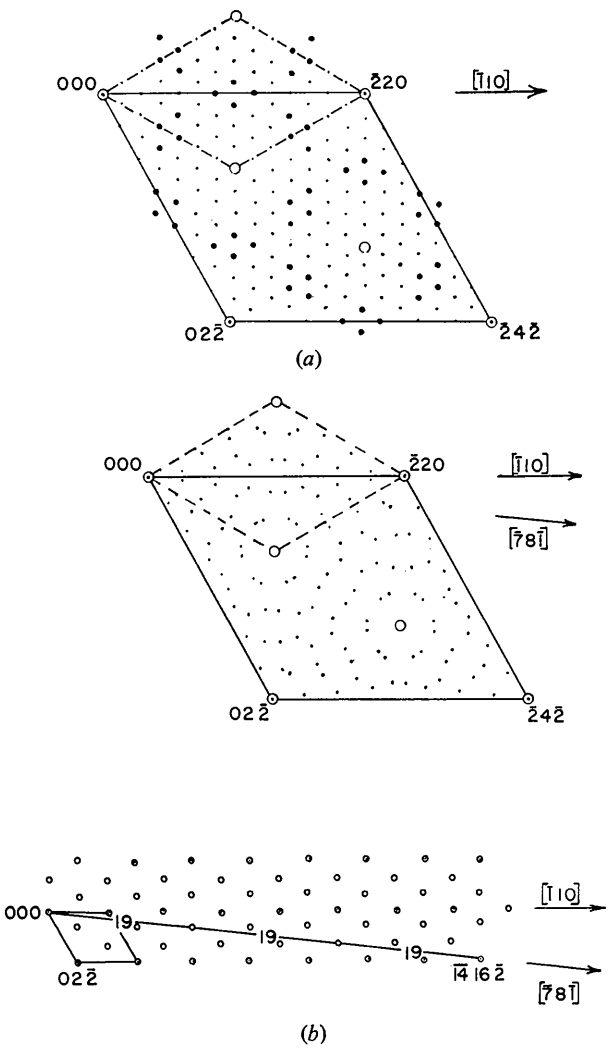


Fig. 5. (*a*) 7th-order diffraction pattern projected onto [111] reciprocal-lattice plane. ⊙ Tri-periodic bulk lattice points on normal rods, ○ other normal rods, ● stronger 7th-order rods, . weaker 7th-order rods. (*b*) 19th-order diffraction pattern projected onto [111] reciprocal-lattice plane. The lower diagram is on a smaller scale to show 57 intervals. ⊙, ○ as in (*a*), . 19th order rods.

For the two specimens polished with $Al_2O_3$ and water, no 19th-order patterns could be produced at all, even though one specimen was heated to the melting point. Strong 7th orders always appeared on cooling below $760 \pm 20$ °C, with a $1 \times 1$ pattern above that temperature. This transition was very sharp and the 7th-order streaks would appear and disappear at 2 second intervals, when the temperature controller was allowed to oscillate about the transition point by $\pm 10$ °C. There appears to be a correlation between the polishing method and which one of the 7th- or 19th-order patterns was obtained by cooling rapidly from a high temperature. One of these structures may require an impurity deposited during the final polishing. No 5th-order pattern as observed by Lander, Gobeli & Morrison (1963) could be formed on any specimen.

A 7th-order pattern is shown in Fig. 2(*f*), with the beam near the $\langle \bar{2}11 \rangle$ azimuth, and the angle of incidence (or tilt angle) set for the 333 Bragg reflection. One can identify Bragg spots from the three dimensional diffraction, streaks from two-dimensional surface effects, bright and dark Kikuchi lines, Kikuchi bands, and thermal-diffuse-scattering spots at the position where Bragg reflections would occur if the crystal were slightly reoriented. The intensities of all of these features are dynamically interrelated. They are easily discerned and can be studied quantitatively, even the thermal-diffuse-scattering spots, which remain separated from the specular (Bragg) spot and the Kikuchi line over a considerable range of angle near the Bragg condition. Similar HEED patterns have been observed by Henderson & Polito (1969).

Planes containing a high density of rods in the reciprocal lattice are revealed as sets of streaks lying on circles where the Ewald sphere intercepts each plane. All of the rods in a unit cell could be located from one photograph if the pattern were recorded out to the first Laue zone, otherwise two or three photographs at different azimuths are required. The rods may then be projected down to find their intercept with the [111] reciprocal lattice plane, as has been done in Fig. 5(*a*) for the 7th-order pattern. The large dots are the consistently more intense of the 7th-order rods, and the open circles are the so-called normal rods which are always present even with a clean and perfect surface. The smaller dotted mesh is primitive.

Fig. 5(*b*) shows the 19th-order streaks similarly projected onto the [111] reciprocal-lattice plane. It is not obvious that any of the 19th-order rods are consistently more intense than the others. There are rapid fluctuations in intensity as the crystal orientation is altered, which is certainly due in part to dynamical interactions, but may also be due to structure along these rods. These projections are very similar to the LEED diffraction patterns for these two structures of Schlier & Farnsworth (1959) and van Bommel & Meyer (1967), but the resolution for the high-energy observations was about an order of magnitude better than for the usual LEED apparatus. The unit meshes for these two structures are

of course identical with those given in the above two references.

### Quantitative intensity recording

The intensity recording apparatus has already been described in Siegel & Menadue (1967). As shown in Fig. 1, a reference signal was taken from a monitor Faraday cup which also defined the ribbon of beam incident on the specimen. This eliminated drifting in the incident beam current density, allowing the data to be accurately recorded as the ratio of the reflected intensity, $I$ to the intensity incident on the specimen, $I_0$. The data were usually taken in logarithmic form, in order to encompass the wide variations in diffracted intensity, of greater than 100 to 1 in some cases. The dimensions of the entrance slit on the main Faraday cup, subtending $5\times10^{-3}$ rad at the specimen normal to its surface, and $5\times10^{-4}$ rad parallel to its surface, were chosen to be just large enough to encompass effectively all of the intensity scattered in a particular streak from these silicon specimens (with the possible exception of the unusually long 222 reflection). The specular spot becomes rather sharp and weak between the Bragg peaks, and the general background scattering contributions significantly to the observed intensity. Thus the depth of the valleys between Bragg peaks in the rocking curves is not quantitatively significant as recorded here, except as a rough indication of general background intensity.

#### (*a*) *The mean inner potential*

The mean inner potential $V_0$ was determined (Table 1) from the refractive shift of the *hhh* reflections towards the shadow edge. It can be shown that for the small angles involved, of less than 5°, it is sufficiently accurate to use $V_0=E(\theta_B-\theta_0)\,(\theta_B+\theta_0)$, where $E$ is the beam voltage, $\theta_B$ the calculated Bragg angle inside the crystal, and $\theta_0$ the measured equivalent vacuum angle of incidence to the net planes. $\theta_0$ was measured at azimuths well away from low-index zone axes to minimize the effects of non-systematic $n$-beam interference, as discussed in the next section on azimuthal plots and by Tull (1951). An average was taken for pairs of azimuths 180° apart to eliminate the effect of the surface being not exactly parallel to the net planes. $\theta_B$ was calculated on the basis of a wavelength $\lambda=0{\cdot}0607\pm2$ Å found by calibrating with a thin Al foil, inserted just before the reflection specimen.

Table 1. *$V_0$ values for the hhh reflections*

| Reflection | 222 | 333 | 444 | 555 |
|---|---|---|---|---|
| $V_0$ | $10{\cdot}9\pm0{\cdot}9$ | $12{\cdot}0\pm0{\cdot}5$ | $11{\cdot}9\pm0{\cdot}6$ | $12{\cdot}0\pm0{\cdot}8$ |
| Reflection | 666 | 777 | 888 | |
| $V_0$ | $12{\cdot}2\pm1{\cdot}2$ | $12{\cdot}4\pm1{\cdot}5$ | $13{\cdot}0\pm2{\cdot}4$ | |

$\langle V_0\rangle=12{\cdot}0\pm0{\cdot}4$

The number of planes $N_e$ effectively contributing to these reflections varies considerably, as shown in Table 2. The two-beam calculations of $N_e$ yields values which are generally too high, nevertheless it is certain that very many atom layers are involved for the 555 and higher-order reflections, so that the average value of $12{\cdot}0\pm0{\cdot}4$ volts for $V_0$ is characteristic of bulk silicon rather than a surface property. The value for the lowest-order reflection is usually found to be low though it is not particularly so in this case. It is susceptible to the slight increase in the separation of the top few atom layers, which decreases $V_0$ directly, and reduces the calculated value still further by decreasing the effective $\theta_B$. There could be a considerable effect also due to a

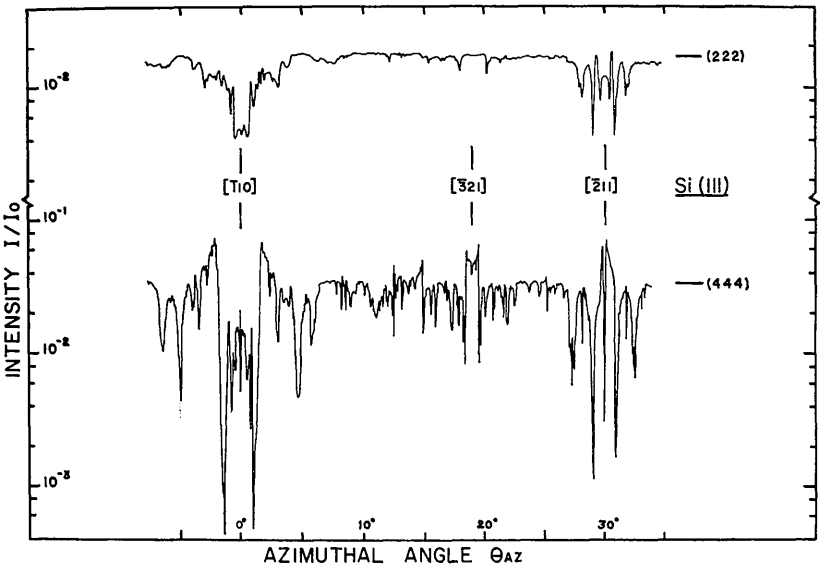


Fig. 6. Azimuthal plots of peak reflected intensity for the 222 and 444 reflections. Intensity fluctuates about an average value, indicated on right.

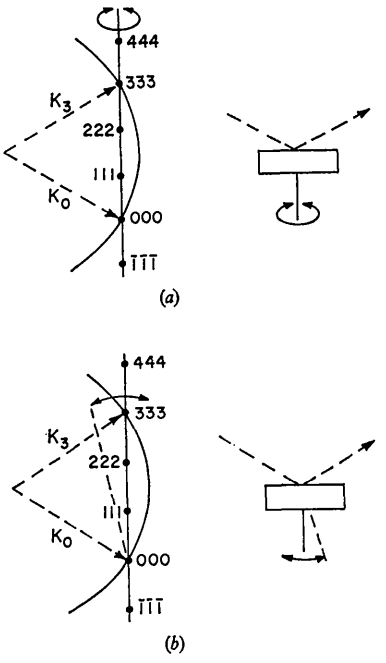


Fig. 7. Geometry of scanning. (*a*) Azimuthal plots, (*b*) rocking curves.

different polarization of the electron charge in and near the surface layer.

Table 2. *Experimental and calculated values for the hhh reflections*

All angles are in milliradians.

| Reflection | 222 | 333 | 444 | 555 | 666 | 777 |
|---|---|---|---|---|---|---|
| $\Delta\theta$obs | 4·26 | 1·86 | 1·00 | 0·66 | 0·66 | 0·60 |
| $\Delta\theta_{2B}$ calc. | – | 1·37 | 0·81 | 0·29 | – | 0·08 |
| $t_e$, Å calc. | – | 8·8 | 13·3 | 35·9 | – | 119 |
| $N_e$, (111) planes | – | 2·8 | 4·2 | 11·4 | – | 38 |

A value of 15·1 volts is calculated from the data of Doyle & Turner (1968) for free atoms. These calculated values are generally found to be higher, and the discrepancy can be ascribed to the change in the wave functions of the outer electrons when the atoms are formed into a lattice.

(*b*) *Azimuthal plots*

For the azimuthal plots, two of which are shown in Fig. 6, the angle of incidence was fixed to satisfy the Bragg condition for the low-order reflections from the net planes parallel to the (111) surface, *i.e.* a systematic set. The total reflected intensity in the neighborhood of each Bragg peak was then recorded as the crystal was rotated about the normal to the reflecting planes. Strong multiple-beam interference caused the observed intensity to fluctuate rapidly at azimuths near low-index zone axes where other reflections were strong, as in the 'Umweganregungen' of the X-ray case. The plots are repeated exactly at every 60° of rotation, and are mirrored at every 30° of rotation, as is to be expected from the symmetry of the crystal.

The degree of complexity of the azimuthal plots increases with the order of reflection. The 222 is the smoothest, and multiple beam interference causes only reductions in intensity. Higher-order reflections are increasingly detailed with both positive and negative fluctuations. It is observed, however, that the fluctuations occur about an obvious average value. The intensity actually rests at this average value when the incident beam azimuth is well away from low index zone axes, so that the 'Umweganregung' interference is minimized. This situation is found visually by observing the Kikuchi pattern. There will be one strong Kikuchi line corresponding to the observed Bragg reflection, but the absence of other low-index Bragg reflections will result in the absence of other Kikuchi lines, either bright or dark, in the neighborhood. Under these conditions, the observed intensity approaches that of the observed Bragg reflection, with multiple beam interference limited to the adjacent systematic reflections, as shown in Fig. 7(*a*). A similar situation occurs in the transmission case (Goodman & Lehmpfuhl, 1967) and the fact that it was found to occur in the Bragg case is important in that it greatly simplifies the *n*-beam calculations.

(*c*) *Rocking curves*

The crystal azimuth was set to one of the several different positions which give the average intensity, fixed there, and the total reflected intensity recorded as a function of the angle of incidence or tilt of the crystal [Fig. 7(*b*)] to obtain a rocking curve. The method is similar to the $\theta$–$2\theta$ method used in X-ray studies. Rocking curves taken this way are consistent in height ($\pm 20\%$) of course, for a particular specimen, and the peak widths are consistent within the experimental error of $\pm 10\%$ for 222 up to 555 reflections. Fig. 8 shows composite rocking curves made over the range of incidence angle from 0·3 to 4°. Each peak was necessarily taken at a different azimuthal angle, but it was found that the detail in the background between the peaks was not sensitive to azimuth either, so that the data overlapped nicely, making a single composite 'azimuth independent' curve possible for each surface structure. In so far as the assumption is correct that only the (111) systematic set of reflections are involved in this data, the peak heights and widths are characteristic of the periodic potential distribution between the (111) planes of the crystal averaged onto the [111] axis.

Both the 222 and 666 reflections would have zero structure factors if the charge distribution about the atoms remained spherical. There is no obvious average intensity value for the 666, and the 666 peak in Fig. 8 has no quantitative significance. It was taken at an arbitrary azimuth to complete the Figure. The 222 on the other hand is consistent and strong. The reflectance peaks at 6% of the incident beam, of which perhaps

3% has an energy loss <4 volts (Colella & Menadue, 1972). Using a simple two-beam calculation, the width at half height of this peak yields a structure factor which is 12 times larger than predicted by a calculation using the X-ray 222 structure factor of Roberto & Batterman (1970), based on covalent bond scattering. The observed strength will be partly due to dynamic interaction with the systematic reflections, particularly the very strong 111 which cannot be observed directly itself because of refraction. For the other peaks the width at half height is not sensitive to the effect of absorption, for the usual ratio of imaginary to real structure potential, $V_g'/V_g \leq 0{\cdot}1$, and it is instructive to compare the full width at half height with the width of the region of total reflection, neglecting absorption. It can be shown that the width of the region of total reflection for the simple two-beam case of the Bragg reflection is given by

$$\Delta\theta_{2B} = \frac{\lambda F_g e^{-M}}{\pi V_c \cos\theta_B \sin\theta_0}$$

where the wavelength $\lambda = 0{\cdot}0607$ Å, $\theta_0$ is the vacuum angle of incidence to the net planes, $V_c$ is the unit-cell volume and $\theta_B$ is the Bragg angle. The structure factors $F_g$ were based on the self consistent field calculations of the scattering factor tabled in Hirsch, Howie, Nicholson, Pashley & Whelan (1965). The Debye–Waller factor $e^{-M}$ was derived assuming a characteristic Debye temperature of 543 °K found for bulk silicon by Batterman & Chipman (1962) with X-ray diffraction.

The two-beam calculated widths are in reasonable agreement with the observed widths for the two lowest order reflections, but become progressively too small for the higher orders. This correlates with the increasing multiple beam interaction, as evidenced by the complexity of the azimuthal plots. Differences in the structure and potential distribution near the surface would, by comparison, affect the lowest order reflections most. They have not been predominant in this case.

(*e*) *Extinction distance*

An estimate can be made of the depth $t_e$, measured perpendicular to the surface, at which the beam intensity has fallen to $1/e$ of its incident strength. By analogy with the discussion for the two-beam X-ray case by Batterman & Cole (1964), at the exact Bragg angle it is found as

$$t_e = \frac{\lambda \sin\theta_B}{2\pi \sin\theta_0 \Delta\theta_{2B}}.$$

These distances will be further reduced by inelastic absorption processes. The calculated values of $t_e$, together with the equivalent number of (111) planes $N_e$, are included in Table 2. It is seen that the energy flow is concentrated very much in the top few atom layers for the low-order Bragg reflections. More accurate values of peak half width $\Delta\theta$ and extinction distance based on *n*-beam calculations will be given in Colella & Menadue (1971).

(*f*) *Temperature effects*

At the azimuths which gave the average intensity as discussed above, the peak reflected intensities, and in one case the integrated intensities were recorded as a function of temperature up to 600 °C. When a $1 \times 1$ or 7 structure was present, the slopes were similar, and in Fig. 9 it can be seen that the peak reflected intensity data fall linearly on a logarithmic intensity scale, as might be expected. When the $\sqrt{19}$ structure was present, the curves exhibited an unexplained break at about 300 °C, becoming steeper above that temperature. The slopes of these logarithmic intensity plots are recorded in °K/decade of intensity in Table 3.

Table 3. *Slopes of the* $1 \times 1$ *and* 7, *and* $\sqrt{19}$ *structures*

All slopes in °K/decade

| Reflection | Slope of $1 \times 1$ and 7 structures | Slopes of $\sqrt{19}$ structure below 300 °C | above 300 °C |
|---|---|---|---|
| 222 | 6000 ± 2000 | 5000 ± 500 | |
| 333 | 2100 ± 250 | 2200 ± 200 | 1200 ± 200 |
| 444 | 1200 ± 150 | 1325 ± 100 | 790 ± 50 |
| 555 | 680 ± 60 | 715 ± 50 | 560 ± 50 |
| 777 | 480 ± 30 | 540 ± 20 | 325 ± 25 |
| 888 | 390 ± 70 | 365 ± 50 | |

The low penetration of the low order reflections (see Table 2) make them particularly interesting. They may be particularly sensitive to surface structure, and there could also be an appreciable effect from the greater freedom of the surface atoms to vibrate under thermal excitation as discussed by Allen & de Wette (1969). The above slopes will be compared with *n*-beam calculations for the bulk structure in another paper (Batterman, Menadue & Colella, 1971).

## Qualitative discussion

The rocking curves taken when the 7 and $1 \times 1$ structures were present were the same in peak heights and

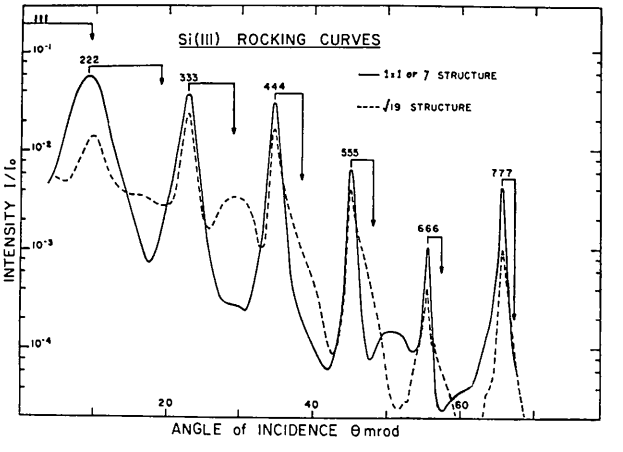


Fig. 8. Si(111) azimuth independent rocking curve. Double arrows indicate shift of each peak owing to refraction at specimen surface.

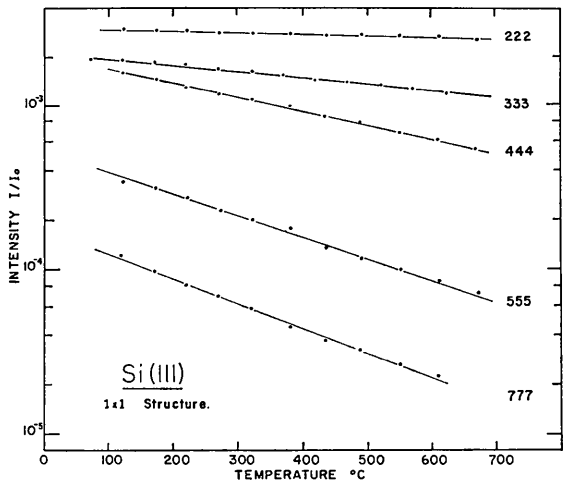

Fig. 9. Peak intensity as a function of temperature.

widths within experimental error, and only slightly different in the detail between the peaks, so only one curve is shown in Fig. 8. This suggests that for these two structures there is very little difference in the average potential distribution in the unit cells, projected onto the normal to the net planes. The periodicity was that of bulk silicon, after correcting for the refractive shift. The 7 structure, as evidenced by the extra streaks in the diffraction pattern may be due to a two-dimensional surface rearrangement of the atoms, involving potential changes in a direction normal to the surface which were too small to be detected here. It is not likely to be a two-dimensional rearrangement of a sub-surface plane, (which would also be consistent with this data) since it would then not be so strongly observed with LEED. The relative intensities of the extra streaks have a characteristic distribution as shown in Fig. 5(*a*) which, it is interesting to note, is similar to that observed by LEED. It is related to the structure within the unit mesh. It is not clear at present whether the 7 structure requires the presence of Fe impurity atoms. Investigators using Auger spectrometry do not agree on this point. Bauer (1968) and Krause (1970) found evidence that Fe was present. On the other hand Taylor (1969) after a careful investigation has concluded that the Auger peaks do not belong to Fe. The 7 structure has also been found to be present immediately after cleaving in a LEED diffraction apparatus, before a significant amount of Fe could have diffused to the surface (Ridgway & Haneman, 1969). In the absence of a detectable impurity, the surface atom rearrangements involving a wrinkling of the surface as discussed by Hansen & Haneman (1969) or periodic absences as discussed by Lander & Morrison (1963) remain as possible explanations. Very light impurity atoms including carbon cannot be ruled out at this stage.

The rocking curve for the $\sqrt{19}$ structure is considerably different from that of the $1 \times 1$ or 7 structures although taken on the same specimen. The bulk silicon peaks are still the strongest features, although the intensities of the 333, 444, and 555 peaks have been reduced by a factor of about 2. The widths at half height of these three reflections remains unchanged. The 222 reflection has been reduced in width by 10%, and in height by a factor of 4, an effect which can be ascribed to the changed surface structure. An outstanding feature is the appearance of a second set of broader and weaker peaks falling very close to the position (marked with arrows in Fig. 8) where silicon Bragg peaks would occur if the mean inner potential were zero. There has clearly been a modification of the structure in a direction normal to the surface. The present specimens were initially cleaned, and repeatedly recleaned by flashing to 1200°C for several seconds, which is long enough to have evaporated tens of monolayers of silicon each time. Considering the ample evidence for the undulating and faceted nature of the surface after such thermal etching (Russell & Haneman, 1967) it is most likely that the present surfaces also undulated. The presence of a predominant area of surface parallel to the (111) net plane is indicated by the consistent refractive shift of the major Bragg peaks, and by the shortness of the streaks. The non-flat areas would then be made up of facets parallel to the net (111) planes, joined by steps or risers.

The simplest explanation of the extra peaks and bumps occurring at the position of silicon peaks, but with negligible refractive shift, would then be that they are due to the penetration of a small part of the incident beam through asperities with sloping entrance and exit faces – the risers mentioned above. The width at half height of the most observable extra peak labelled 333 in Fig. 8 was a considerable $7 \times 10^{-3}$ rad, which corresponds to an average window height, set by the riser, of 9 Å. This is just 3 times the 111 plane spacing. The surface would have to have many such asperities (occurring perhaps as the topmost steps on an undulating surface), which were short enough in the direction of the beam to be penetrated. The conditions under which the $\sqrt{19}$ structure is formed, of rapid cooling from a temperature near the melting points would also favour the presence of an increased number of small steps, due to the rapid evaporation of about 10 monolayers during the flashing.

The presence of nickel on surfaces displaying the $\sqrt{19}$ structure has been consistently observed (van Bommel & Meyer, 1967; Bauer, 1968). Indeed quantitative Auger spectrometry by Taylor (1969) has found sufficient nickel to constitute close to a monolayer of nickel silicide. The presence of the nickel may well be the factor which determines that a sufficient number of small steps form to be observed by beam penetration. Annealing at temperatures above 570°C caused the 19th-order pattern to fade, probably by the nickel dissolving into the silicon. Simultaneously, the steps have become too few and the asperity thickness too great for asperity penetration to be significant. *In situ* replication of the various surfaces would verify this qualitative explanation directly.

## Conclusions

The undulatory nature of the surface did not change appreciably as the surface was cleaned, or one surface structure converted to another. The measured peak intensities were well reproduced for a given specimen, for each surface structure when it was reformed. Thus the relative intensities for different surface structures could be compared. The azimuth independent rocking curves, taken under conditions of minimized non-systematic 'Umweganregung' were found to differ strongly for the $\sqrt{19}$ structure compared to either the 7 or the $1 \times 1$ structures. The lowest order 222 reflections was reduced by a factor of 4. The width of this peak would suggest that the energy flow was concentrated in the upper few atom layers, and the large reduction in intensity may reflect a considerable structural change. The 7 and $1 \times 1$ structures were identical within the experimental accuracy, in peak heights and widths, and could not be resolved by this means.

The peak intensities of the higher order reflections, the 333 up to the 555, were reproducible within $\pm 20\%$ on a given specimen, provided it was not flashed near the melting point too often, which caused a gradual lessening of intensity. The contribution of the surface structure to these reflections becomes rapidly less important as the penetration increases at higher angles of incidence. Thus the higher order peak intensities and widths, and their variation with temperature, are suitable for comparison with an *n*-beam dynamical theory for the Bragg case in the crystal bulk, and the calculations may be initially based on a simple semi-inifinite model for the crystal surface.

As seen in the last section, extra peaks will occur if a sufficient part of the beam can penetrate through asperities. Fortunately for the lower-order Bragg reflections the extra peaks produced in this way are displaced far enough to be separately resolvable, owing to the absence of refractive shift. This simplifies quantitative measurements.

Surface non-flatness must be a prime consideration. It will obviously always be an important factor at glancing angles of incidence. As discussed in Cowley & Warburton (1969) it may be possible to include the effects of some types of surface non-flatness in the calculations. The surface topography obviously has a strong influence on the length of crystal which the Bragg scattered beam must traverse before entering the vacuum, and the gross effects of this will be discussed in Colella & Menadue (1972).

It has been shown that the glancing incidence high energy technique is particularly appropriate to the study of the topological as well as the structural periodic changes occurring on single crystal surfaces under ultra high vacuum conditions.

The author is indebted to Professor B. W. Batterman for his continued interest in this work and for many stimulating discussions. This work was made possible through a grant from the Air Force Office of Scientific Research (AF-AFOSR-1652-69) and was aided by the support facilities of the Materials Science Center at Cornell University.

## References

ABBINK, H. C., BROUDY, R. M. & MCCARTHY, G. P. (1968). *J. Appl. Phys.* **39**, 4673.
ALLEN, F. G., EISINGER, J., HAGSTROM, H. D. & LAW, J. J. (1959). *J. Appl. Phys.* **30**, 1563.
ALLEN, R. E. & DE WETTE, F. W. (1969). *Phys. Rev.* **188**, 13320.
BATTERMAN, B. W. & CHIPMAN, D. R. (1962). *Phys. Rev.* **127**, 690.
BATTERMAN, B. W. & COLE, H. (1964). *Rev. Mod. Phys.* **36**, 681.
BATTERMAN, B., MENADUE, J. & COLELLA, R. (1971). To be published.
BAUER, E. (1968). *Phys. Letters* A**26**, 530.
BOMMEL, A. J. VAN, & MEYER, F. (1967). *Surface Sci.* **8**, 473.
COLELLA, R. (1972). *Acta Cryst.* A**28**,11.
COLELLA, R. & MENADUE, J. (1972). *Acta Cryst.* A**28**, 16.
COWLEY, J. M. (1967). *Progr. Mater. Sci.* **13**, No. 6, 269.
COWLEY, J. M. (1969). *Acta Cryst.* A**25**, 129.
COWLEY, J. M. & WARBURTON, P. M. (1969). In *The Structure and Chemistry of Solid Surfaces*. Edited by G. A. SOMERJAI, New York: John Wiley.
DOYLE, P. A. & TURNER, P. S. (1968). *Acta Cryst.* A**24**, 390.
FINCH, G. I. & WILMAN, H. (1937). *Ergebn. exakt. Naturw.* SVI, p. 353.
GOODMAN, P. & LEMHPFUHL, G. (1967). *Acta Cryst.* **22**, **14**.
HANSEN, N. R. & HANEMAN, D. (1964). *Surface Sci.* **2**, 566.
HENDERSON, R. C. & POLITO, W. J. (1969). *Surface Sci.* **14**, 473.
HENDERSON, R. C., POLITO, W. J. & SIMPSON, J. (1970). *Appl. Phys. Letters*, **16**, 15.
HIRSCH, P. B., HOWIE, A., NICHOLSON, R. B., PASHLEY, D. W. & WHELAN, M. J. (1965). *Electron Microscopy of Thin Crystals*. London: Butterworths.
JONES, R. O. & STROZIER, J. A. (1969). *Phys. Ref. Letters*, **22**, 1186.
KATO, N. (1952). *Phys. Soc. Japan*, **7**, 406.
KRAUSE, G. O. (1970). VII *Intern. Congr. Electron Microscopy Grenoble*, p. 297.
LANDER, J. J., GOBELI, G. W. & MORRISON, J. (1963). *J. Appl. Phys.* **34**, 2298.
LANDER, J. J. & MORRISON, J. (1963). *J. Appl. Phys.* **34**, 1403.
MENADUE, J. & SIEGEL, B. M. (1969). In *The Structure and Chemistry of Solid Surfaces*. Edited by G. A. SOMERJAI. New York: John Wiley.
MILLER, D. P., WATELSKI, S. B. & MOORE, R. C. (1964). *J. Appl. Phys.* **34**, 2813.
MIYAKE, S. & HAYAKAWA, K. (1970). *Acta Cryst.* A**26**,60.
NEWMAN, R. C. & PASHLEY, D. W. (1955). *Phil. Mag.* **7**, 927.
RIDGWAY, J. W. T. & HANEMAN, D. (1969). *Appl. Phys. Letters*, **14**, 265.

ROBERTO, J. B. & BATTERMAN, B. W. (1970). MSC Report No. 1357, Cornell Univ.
RUSSELL, G. J. (1970). *Surface Sci.* **19**, 217.
RUSSELL, G. J. & HANEMAN, D. (1967). *J. Electrochem. Soc.: Solid State Sci.* **114**, 398.
SCHLIER, R. E. & FARNSWORTH, H. E. (1959). *J. Chem. Phys.* **30**, 917.
SEWELL, P. B. (1970). Private communication.
SIEGEL, B. M. & MENADUE, J. F. (1967). *Surface Sci.* **8**, 206.
STROZIER, J. A. & JONES, R. O. (1970). MSC Report No. 1363, Cornell Univ.
TAYLOR, N. (1969). *Surface Sci.* **15**, 169.
TULL, V. F. G. (1951). *Proc. Roy. Soc.* A**206**, 219.
VAINSHTEIN, B. K. (1964). *Structure Analysis by Electron Diffraction.* Oxford: Pergamon.

*Acta Cryst.* (1972). A**28**, 11

# *n*-Beam Dynamical Diffraction of High-Energy Electrons at Glancing Incidence. General Theory and Computational Methods*

BY R. COLELLA†

*Department of Materials Science and Engineering, Cornell University, Ithaca, New York* 14850, *U.S.A.*

(*Received* 9 *October* 1970)

The *n*-beam dynamical theory of high-energy electrons is currently used in transmission (Laue case) for accurate determination of the Fourier components of the crystal potential. The same theory is expected to provide information about the surface potential when used to interpret diffraction patterns in reflection at glancing incidence (Bragg case). Some peculiar aspects are elucidated in detail, insofar that they are different from the transmission case, particularly the boundary conditions. Inelastic scattering effects are introduced by means of a complex potential. Changes of the Fourier components of the potential near the surface are considered, and a model has been developed which incorporates these changes into the theory. A slice treatment developed in the frame of Bethe's theory is presented.

## 1. Introduction

Diffraction of electrons from a flat surface of a single crystal has been widely used in the last few years for surface investigations. When the energy of the primary beam is of the order of a few keV (high-energy electron diffraction, HEED) the actual penetration of the electron beam is much higher than in low-energy electron diffraction (LEED), but owing to the small grazing angle (of the order of 1 to 3°), it is to be expected that a HEED diffraction pattern will reflect the properties of the first few atomic layers. This is confirmed by the streaky character of the diffraction spots observed at different stages during heat treatment in the case, for instance, of tungsten (Siegel & Menadue, 1967).

The essential tool for understanding a HEED pattern from a quantitative point of view is of course the *n*-beam dynamical theory such as that developed for the transmission case (Laue case) (Hirsch, Howie, Nicholson, Pashley & Whelan, 1965).* In transmission experiments the *n*-beam dynamical theory has been successfully used for the accurate determination of structure factors (Cowley, 1969), in the frame of a scattering theory based upon the first Born approximation. Within the limits of such an approximation it is permissible to express the Fourier components of the crystal potential in terms of the scattering cross section for each atom within the crystal cell, a kinematic approximation being made within each cell. Such an approximation, to be sure, is not permissible in LEED.

It is expected, in principle, that the same theory applied to the Bragg case should be able to give information on the surface charge density *via* the atomic potential.

Although the basic formalism of the *n*-beam dynamical theory for the Bragg case is essentially the same as for the Laue case, there are some differences in the practical developments of the calculations, especially as far as the boundary conditions are concerned.

This paper will give a description of how the *n*-beam dynamical theory for electrons has been applied to the Bragg case of diffraction. It will be shown in detail how the original theory developed by Bethe (1928) has been used for this purpose.

A model will be described in which possible changes of the crystal inner potential can be taken into account in the frame of such a theory. Rocking curves (reflectivity *vs.* angle of incidence) have been computed in

* Work supported by the Air Force Office of Scientific Research.

† Present address: Department of Physics, Purdue University, Lafayette, Indiana 47907, U.S.A.

* Diffraction theory is an alternative but equivalent approach to band theory, as pointed out by Stern, Perry & Boudreaux (1969). *E vs. k* plots are replaced here by the dispersion hypersurface.